Rosenberg, T. (1964) *Arch. Biochem. Biophys. 105*, 315-322.
Shindo, H. (1980) *Biopolymers 19*, 509-522.
Sperling, J. E., Feldmann, K., Meyer, H., Jahnke, U., & Heilmeyer, L. M. G. (1979) *Eur. J. Biochem. 101*, 581-592.
Sundralingam, M., & Putkey, E. F. (1970) *Acta Crystallogr., Sect. B B26*, 790-800.
Terao, T., Matsui, S., & Akasaka, K. (1977) *J. Am. Chem. Soc. 99*, 6136-6138.
Vogel, H. J., & Bridger, W. A. (1981) *Biochem. Soc. Trans. 9*, 159.
Withers, S. G., Madsen, N. B., & Sykes, B. D. (1981) *Biochemistry 20*, 1748-1756.
Wolodko, W. T., Brownie, E. R., & Bridger, W. A. (1980) *J. Bacteriol. 143*, 231-237.
Yguerabide, J., Epstein, H. F., & Stryer, L. (1970) *J. Mol. Biol. 51*, 573-590.

Resonance Raman Investigation of Carbon Monoxide Bonding in (Carbon monoxy)hemoglobin and -myoglobin: Detection of Fe–CO Stretching and Fe–C–O Bending Vibrations and Influence of the Quaternary Structure Change†

Motonari Tsubaki,‡ Raja B. Srivastava, and Nai-Teng Yu*

ABSTRACT: We report for the first time the direct identification of the iron–carbon bond in (carbon monoxy)hemoglobins (HbCO) and -myoglobin (MbCO) by resonance Raman spectroscopy. The Fe–CO stretching, Fe–C–O bending, and bound C–O stretching vibrations have been detected at 507 (512), 578 (577), and 1951 (1944) cm^{-1}, respectively, in human (carbon monoxy)HbA (sperm whale MbCO) upon excitation at 406.7 nm within the Soret band. These assignments were made on the basis of frequency shifts with the isotopes $^{13}C^{16}O$, $^{12}C^{18}O$, and $^{13}C^{18}O$. Calculated isotope shifts according to the model Im–Fe–C–O (but not Im–Fe–O–C) agree well with the observed data. The possible mechanisms of resonance Raman enhancement of these vibrations are discussed in terms of the $d_\pi(Fe)$–$\pi^*(CO)$ interaction. Careful examination of the Fe–CO stretching mode at 507 cm^{-1} (ρ = 0.055) in both (carbon monoxy)HbA and (carbon monoxy)Hb Kansas with and without inositol hexaphosphate (IHP) reveals no changes in frequency and intensity. This implies that no significant change in the Fe–C bond energy is induced by switching the quaternary structure from the R to the T form in ligated (carbon monoxy)Hb Kansas. The absence of bond tension between the iron atom and the proximal histidine is suggested, as it has been demonstrated that the ν(Fe–CO) frequency is sensitive to a change from 1-methylimidazole to 1,2-dimethylimidazole (as fifth ligand) in model heme–CO complexes. However, the resonance Raman spectrum of carp (carbon monoxy)Hb exhibits a broadening of the Fe–CO stretching mode on the lower energy side upon R → T conversion with IHP, suggesting the presence of a new conformer (or conformers) with a weaker Fe–CO bond or a somewhat different CO distortion.

Carbon monoxide, a competitive inhibitor for oxygen-binding hemoproteins, is a useful probe for heme environment around the distal site. Unlike dioxygen, it is incapable of oxidizing the heme. The bound CO stretching vibration, ν(C–O), can be readily detected by infrared (IR) spectroscopy. Carbon monoxide bound to hemoglobin A (HbA) shows a sharp single absorption band at 1951 cm^{-1} (Alben & Caughey, 1968), whereas in human hemoglobin variants, Hb Zürich (63 E7 His → Arg) exhibits its bound ν(C–O) at 1958 (β) and 1951 (α) cm^{-1}, and (carbon monoxy)HbM Emory (63 E7 His → Tyr) absorbs at 1970 (β) and 1951 (α) cm^{-1} (Caughey et al., 1969; Tucker et al., 1978). Thus, the substitution of distal His E7 by other amino acid residues alters the ν(C–O) frequency in the mutant subunits but not in the normal subunits. More interesting is the observation of multiple ν(C–O) frequencies (1933, 1944, and 1967 cm^{-1}) in the IR spectrum of the monomeric CO complex of sperm whale myoglobin, which was interpreted as indicating three different heme–carbonyl conformers in the same heme cavity (Makinen et al., 1979), although only one conformer has been reported in crystals by neutron diffraction studies (Norvell et al., 1975).

Unlike infrared spectroscopy, detection of axial ligand vibrations by resonance Raman scattering of hemoproteins in dilute aqueous solution is not restricted to the narrow "window" region because water is a weak Raman scatterer (Yu, 1977). In fact, several iron–ligand stretching vibrations such as Fe(II)–O_2, Fe(II)–NO, Fe(III)–OH, Fe(III)–N_3, and Fe(III)–CN have been identified by resonance Raman spectroscopy with the ligand isotope substitution technique (Brunner, 1974; Chottard & Mansuy, 1977; Asher et al., 1977; Tsubaki et al., 1981; M. Tsubaki and N. T. Yu, unpublished results). Moreover, internal ligand vibrations can also be resonance enhanced by tuning the excitation wavelength into a responsible charge-transfer band (Wright et al., 1979; Tsubaki et al., 1981; Yu & Tsubaki, 1980).

Thus, resonance Raman spectroscopy appears to be a powerful technique to study the direct interactions between the heme and its axial ligands. However, its application to (carbon monoxy)hemoglobins or -myoglobins has been limited to pulse laser transient kinetic studies (Woodruff & Farquharson, 1978; Dallinger et al., 1978; Lyons et al., 1978; Coppey et al., 1980; Friedman & Lyons, 1980; Terner et al., 1980), although a preliminary work using continuous wave (CW) laser excitation

† From the School of Chemistry, Georgia Institute of Technology, Atlanta, Georgia 30332. *Received June 1, 1981.* This research was supported by Grant GM 18894 from the National Insitutes of Health. N.-T.Y. is the recipient of a National Institutes of Health Research Career Development Award (EY 00073).

‡ Present address: Department of Biochemistry, Kagawa Medical School, Kagawa 761-07, Japan.

0006-2960/82/0421-1132$01.25/0

was reported by Rimai et al. (1975). Identification of ν(Fe–CO) has been difficult because carbon monoxide dissociates from heme easily upon illumination of laser light, generating deoxy species which interfere with the observation of signals from unphotolyzed complexes.

In this paper, we demonstrate the feasibility of obtaining high-quality resonance Raman spectra of HbCO and MbCO which contain negligible contributions from photolyzed deoxy species. With the excitation wavelength at 406.7 nm, two Raman lines at 507 (512) and 578 (577) cm^{-1} in HbCO (MbCO) are sensitive to CO isotope substitution. On the basis of a linear Fe–C–O configuration (tilted away from the heme normal by ~13°) as revealed by the X-ray crystallographic studies of human (carbon monoxy)HbA (at 2.7-Å resolution) (Baldwin, 1980), the pattern of observed isotope shifts and normal coordinate calculations permit us to establish that the most intense line at 507 (512) cm^{-1} (in the 100–650-cm^{-1} region) is the ν(Fe–CO) stretching, and the weaker one at 578 (577) cm^{-1} is a δ(Fe–C–O) bending mode. We also observed resonance enhancement of the bound ν(C–O) vibration at 1951 (1944) cm^{-1} in HbCO (MbCO) in agreement with those observed by infrared spectroscopy. In addition, we report a significant broadening of the ν(Fe–CO) line in carp HbCO upon quaternary structure change from R to T.

Materials and Methods

Preparation of Proteins. Sperm whale myoglobin (Sigma) was purified in the carbon monoxy form as described previously (Tsubaki et al., 1981). Human hemoglobin A (HbA) was prepared in the oxy form by the usual procedure from whole blood (Kilmartin et al., 1975) and then was converted to the carbon monoxy form. Carp Hb was kindly donated by Dr. R. W. Noble and was prepared from washed red blood cells by lysis (Tan et al., 1972). Because considerable amounts of oxidized carp Hb were formed during transportation, complete reduction of carp Hb was performed by using sodium dithionite under a carbon monoxide atmosphere followed by anaerobic gel filtration (Sephadex G-25, Whatman) to form carp HbCO. Separation of each carp Hb fraction was performed by the method of Tan et al. (1972) with slight modification. Carp Hb hemolysate in the carbon monoxy form was charged onto a DEAE-cellulose (DE-52, Whatman) column, 2 × 20 cm, equilibrated with 0.002 M sodium borate buffer, pH 9.0. The fractions were eluted by a linear gradient of borate concentration at pH 9.0 at 4.0 °C, the starting buffer being 1 L of 0.002 M sodium borate and the final buffer being 1 L of 0.020 M sodium borate buffer. The flow rate was 30 mL/h, and all the buffers used for fractionation had been bubbled by carbon monoxide gas to avoid the oxidation of heme. Hb Kansas was a kind gift from Dr. K. Nagai. All the hemoglobin samples used were gel filtered against 1 mM Na_2HPO_4 and deionized by passage through a Dintzis column (Nozaki & Tanford, 1967).

Preparation of Carbon Monoxy Derivatives. Hb (or Mb) solution was diluted with an appropriate buffer and transferred into a cylindrical quartz Raman cell with rubber septum. The solution was deoxygenated by repeated evacuation and flushing of pure nitrogen, and then carbon monoxide gas was introduced to ensure that all hemes were saturated with CO. This procedure is necessary because residual oxygen in the solution could replace the carbon monoxide upon laser illumination. The quantum yield for photodissociation of carbon monoxide derivatives is much higher than those of oxygenated hemoproteins. Extreme care was taken to avoid the formation of oxidized heme in solution especially at low pH, which may affect the Raman spectrum significantly because of the closer proximity of the Soret maxima of oxidized derivatives to the excitation wavelength. The extent of oxidation can be estimated from Raman spectra in both higher frequency (1200–1700 cm^{-1}) and lower frequency (100–700 cm^{-1}) regions. Although the spectra were compared with and without sodium dithionite under an atmosphere of carbon monoxide gas, we could not observe any difference between them.

Carbon monoxide was obtained from the following manufacturers: $^{12}C^{16}O$ from Matheson (CP grade), $^{13}C^{16}O$ from Bio-Rad (93.1 atom % ^{13}C), and $^{12}C^{18}O$ and $^{13}C^{18}O$ from Prochem (99.0 atom % ^{18}O, 91.7 atom % ^{13}C, and 98.5 atom % ^{18}O, respectively).

Measurement of Raman Spectra. The Raman cell (diameter 1.95 cm) was kept in a rotating (~2000 rpm) cell holder for laser irradiation to avoid local heating and to reduce the photodissociation, and a 90° scattering geometry was used to obtain Raman spectra at room temperature. Under the spinning condition, the time required for the sample to pass through a 20-μm laser beam is $\sim 10^{-5}$ s. The 406.7-nm emission of a krypton ion laser (Spectra-Physics Model 171-01) was employed for excitation, and the laser power was maintained at 10 mW at sample point unless otherwise stated. The scattered light was analyzed by using a multichannel Raman system which consists of a dry ice cooled silicon-intensified target (SIT) detector, a detector controller, a microprocessor-based OMA 2 console (PAR 1215), and a Spex 1402 0.85-m Czerny-Turner double monochromator. This Raman system has been described in detail previously (Yu & Srivastava, 1980). All the wavenumbers reported here are accurate to ±1 cm^{-1} for sharp lines and ±2 cm^{-1} for broad lines.

Results

High-Frequency Region Spectra. In Figure 1 are presented two sets of Raman spectra in the 1250–1750-cm^{-1} region: the first set (curves 1 and 2) for (carbon monoxy)HbA and the second set (curves 3 and 4) for (carbon monoxy)Mb. Curves 1 and 3 were obtained with a lower laser power (~6 mW) than curves 2 and 4 (~15 mW). With increasing laser power, intensity increases at 1357 (1357), 1471 (1472), and 1566 (1565) cm^{-1} in the spectra of (carbon monoxy)HbA (MbCO) whereas the 1586-cm^{-1} line shows an intensity reduction. These Raman intensity changes are due to the formation of deoxy-HbA (deoxy-Mb) caused by partial photodissociation of bound CO. The deoxy-HbA spectrum (Figure 2, upper panel) excited at the same wavelength supports this interpretation; the 1587-cm^{-1} line disappears, and the 1358- and 1473-cm^{-1} lines are dominant in the spectrum. Since the quantum yields for photodissociation of (carbon monoxy)Mb (0.97) and (carbon monoxy)HbA (0.46) are high, significant amounts of deoxy derivatives are expected to be formed upon laser irradiation (Stanford et al., 1980; Noble et al., 1967; Sawicki & Gibson, 1979). However, closer proximity of the excitation wavelength (406.7 nm) to the Soret band maxima of the carbon monoxy derivatives than to those of the deoxy derivatives gives rise to much stronger Raman scattering intensity in the region below 700 cm^{-1} for carbon monoxy derivatives. With the assumption that the Soret band maxima are very close to the 0–0 origin, the theories of resonance Raman scattering intensity (Felton & Yu, 1978) predict somewhat enhanced intensity for deoxy-HbA Raman modes in the 1300–1700-cm^{-1} region because these modes are expected to have their 0–1 excitation profile maxima at ~406.7 nm.

Resonance Raman spectra of (carbon monoxy)HbA (Figure 1, curve 1) and oxy-HbA (Figure 2, lower panel) in the 1250–1750-cm^{-1} region exhibit both similarities and differ-

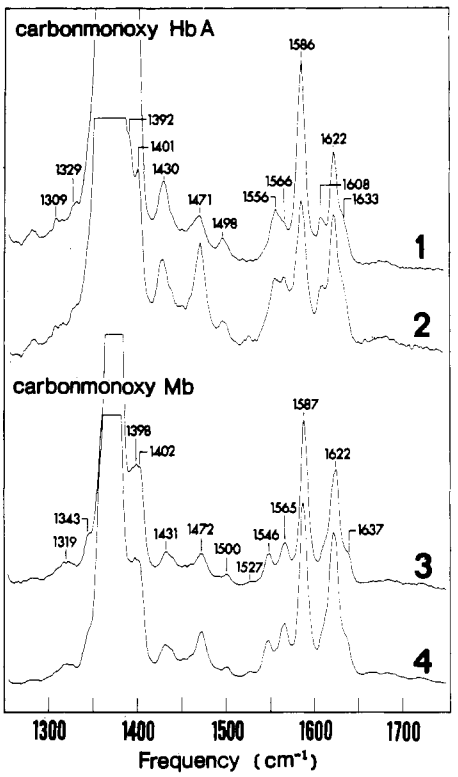

FIGURE 1: Higher frequency region (1250–1750 cm^{-1}) spectra of (carbon monoxy)HbA (upper portion) and (carbon monoxy)Mb (lower portion). Conditions were the following: excitation wavelength, 406.7 nm; laser power, 5, 20, 7.5, and 12.5 mW at the sample in descending order (curves 1 → 4); slit width, 100 μm; slit height, 0.2 cm; delay, 10000 (303 s). Sample conditions were ~60 μM (carbon monoxy)HbA or -Mb (heme basis) in 0.05 M Tris-HCl, pH 8.4, buffer.

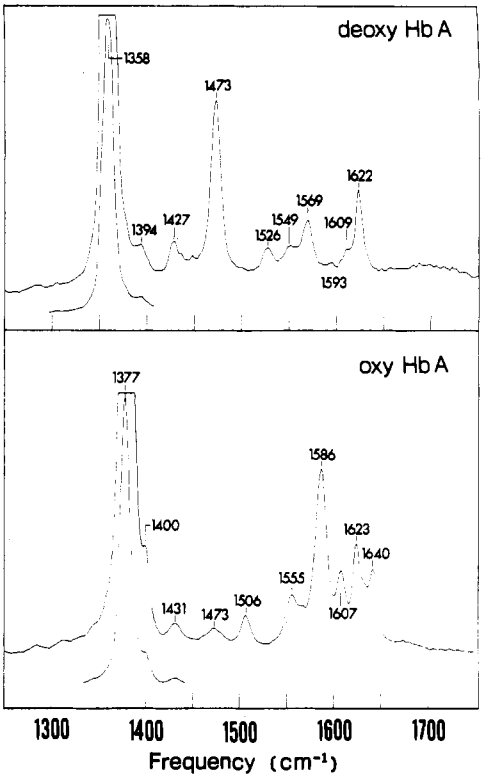

FIGURE 2: Higher frequency region (1250–1750 cm^{-1}) spectra of deoxy-HbA (upper panel) and oxy-HbA (lower panel). Conditions are the same as in Figure 1, except for the excitation laser powers which are 15 mW for deoxy-HbA and 18 mW for oxy-HbA.

ences. The most noticeable differences occur at 1498 → 1506, 1633 → 1640, and 1372 → 1377 cm^{-1}.

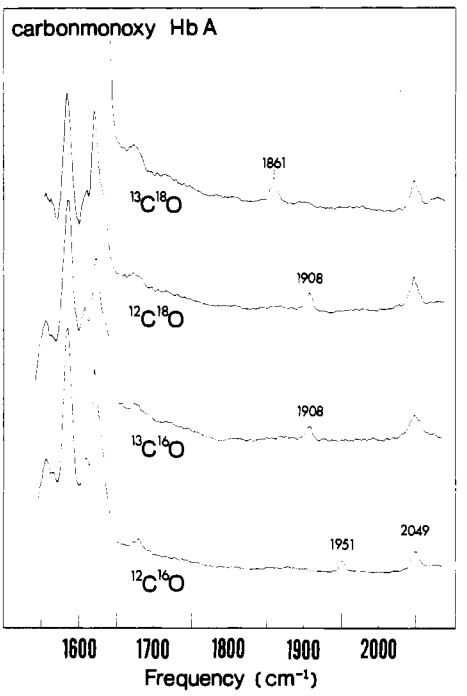

FIGURE 3: Carbon monoxide isotope effects on higher frequency region (1500–2100 cm^{-1}) spectra of (carbon monoxy)HbA. The spectra are arranged in the order of masses of carbon monoxide isotopes. Conditions are the same as in Figure 1 except for the excitation laser power, which is 10 mW.

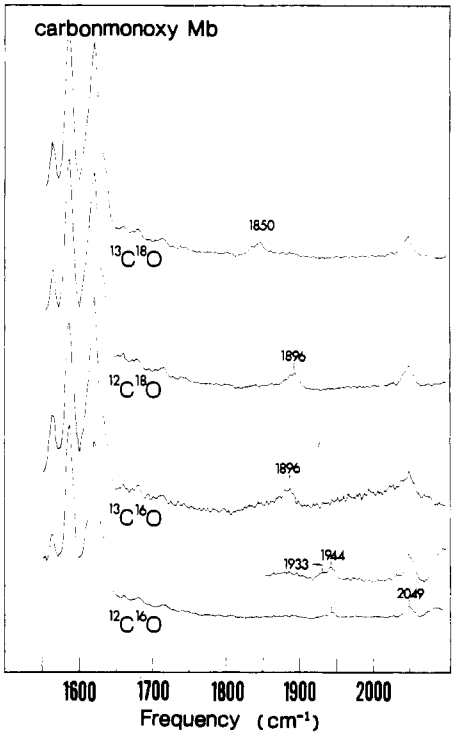

FIGURE 4: Carbon monoxide isotope effects on higher frequency region (1500–2100 cm^{-1}) spectra of (carbon monoxy)Mb. The spectra are arranged in the order of masses of carbon monoxide isotopes. Conditions are the same as in Figure 1 except for the excitation laser power, which is 10 mW.

Detection of Bound C–O Stretch. The bound CO internal stretching vibration of (carbon monoxy)HbA was detected as a single line as shown in Figure 3. Its frequency shifts from 1951 ($^{12}C^{16}O$) to 1908 ($^{13}C^{16}O$), 1908 ($^{12}C^{18}O$), and 1861 cm^{-1} ($^{13}C^{18}O$). The first three frequencies are in good agreement with the results obtained by infrared spectroscopy (Alben &

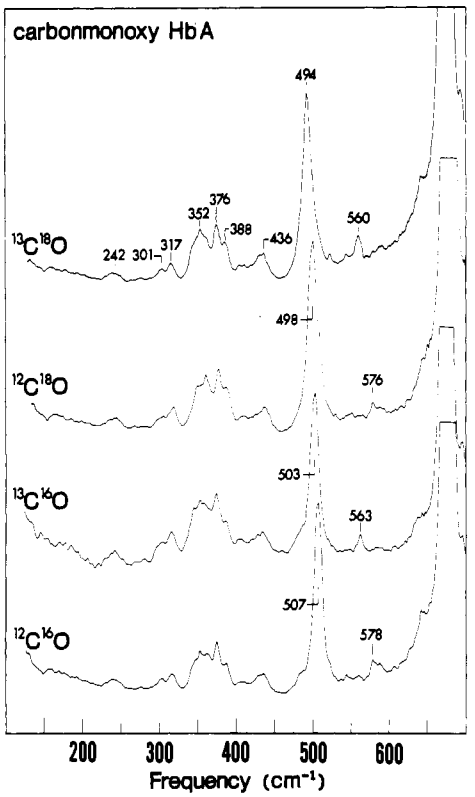

FIGURE 5: Carbon monoxide isotope effects on lower frequency region (100–700 cm^{-1}) spectra of (carbon monoxy)HbA. The spectra are arranged in the order of masses of carbon monoxide. Other conditions are the same as in Figure 1.

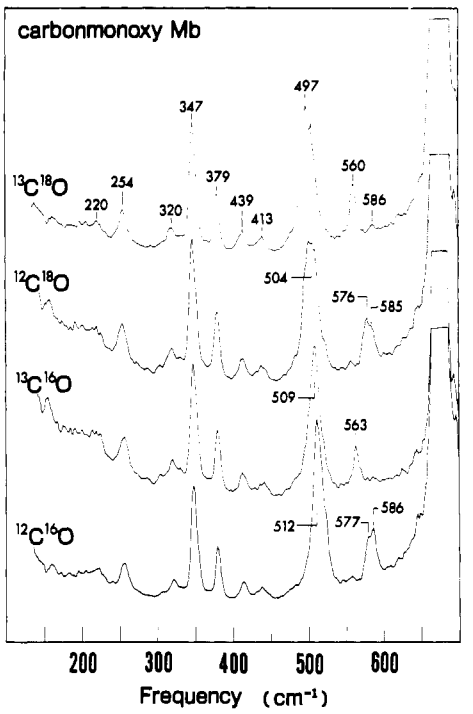

FIGURE 6: Carbon monoxide isotope effects on lower frequency region (100–700 cm^{-1}) spectra of (carbon monoxy)Mb. The spectra are arranged in the order of masses of carbon monoxide isotopes. Other conditions are the same as in Figure 1.

Caughey, 1968; Caughey et al., 1969; Satterlee et al., 1978). The corresponding spectra for sperm whale (carbon monoxy)Mb are shown in Figure 4, where the main ν(C–O) stretch appears at 1944 cm^{-1} with a shoulder near 1933 cm^{-1} in the spectrum of Mb^{12}C^{16}O. Upon isotope substitution, the main ν(C–O) stretch shifts to 1896 cm^{-1} (both ^{13}C^{16}O and ^{12}C^{18}O) and 1850 cm^{-1} (^{13}C^{18}O), all of them with a shoulder at the lower frequency side.

Detection of Fe–CO Stretch and Fe–C–O Bending Frequencies. Lower frequency region spectra of deoxy-HbA and -Mb excited at 406.7 nm are extremely weak and featureless except for lines around 220 cm^{-1} which have been assigned as an Fe–N$_\epsilon$(His F8) stretching vibration in the deoxy state (Nagai et al., 1980a). The Raman scattering cross section of the deoxy species is far smaller than that of the carbon monoxy derivatives. Indeed, lower frequency region (100–700 cm^{-1}) spectra of (carbon monoxy)HbA and -Mb are almost independent of excitation laser power (10–40 mW). The lower frequency region spectrum of HbA^{12}C^{16}O is dominated by the appearance of a sharp and polarized line at 507 cm^{-1} (ρ = 0.055) (Figure 5), which was noticed by Rimai et al. (1975) with near-Soret excitation (441.6 nm) although they interpreted it as a porphyrin ring mode corresponding to the 485-cm^{-1} line in oxy-HbA. However, carbon monoxide isotope substitution experiments revealed clearly that this line exhibits a monotonous frequency shift toward lower energy with the mass of carbon monoxide increasing from ^{12}C^{16}O to ^{13}C^{18}O (Figure 5). In addition, we noticed another isotope-sensitive line with much weaker intensity at 578 cm^{-1} for HbA^{12}C^{16}O, which shifts to 563 cm^{-1} upon substitution by ^{13}C^{16}O, to 576 cm^{-1} by ^{12}C^{18}O, and to 560 cm^{-1} by ^{13}C^{18}O.

In the spectra of (carbon monoxy)Mb (Figure 6), the two isotope-sensitive lines appear at 512 and 577 cm^{-1}. The one at 512 cm^{-1} shows a monotonous frequency shift toward lower energy, whereas the one at 577 cm^{-1} shows "zigzag" frequency shifts in the order ^{12}C^{16}O → ^{13}C^{16}O → ^{12}C^{18}O → ^{13}C^{18}O.

For the Fe–CO stretching vibration, the carbon and oxygen atoms can be treated as a dynamic unit because the C–O stretching force constant is much larger than the Fe–C stretching force constant. Thus, one would expect that the Fe–CO stretching frequency is simply dependent on the sum of the masses of both carbon and oxygen. Indeed, this appears to be the case for the line at 507 (HbA^{12}C^{16}O) or 512 cm^{-1} (Mb^{12}C^{16}O). On the other hand, for an Fe–C–O bending mode, the amplitude of vibration of the bound carbon is far greater than that of the terminal oxygen, since the moments of oscillation of these two atoms around the much heavier iron atom must approximately cancel. Therefore, one would predict that the effects of isotope substitution for terminal oxygen upon δ(Fe–C–O) frequency can be relatively small if compared to those for bound carbon. Accordingly, the Raman lines at 578 cm^{-1} for HbA^{12}C^{16}O and at 577 cm^{-1} for Mb^{12}C^{16}O are assignable to an Fe–C–O bending mode.

To confirm our assignments, we have carried out a normal coordinate analysis based on the simplified model imidazole–Fe–C–O. The porphyrin ring was neglected in this model because the porphyrin plane is assumed to be perpendicular to the plane containing the fifth and sixth ligands of iron, i.e., imidazole and carbon monoxide. It is further assumed that the out-of-plane porphyrin ring mode is not significantly coupled with ligand-related vibrations. Imidazole was treated as a single dynamical unit with a mass of 68 amu. The structural parameters used in this model are as follows: r(Fe–Im) = 2.00 Å, r(Fe–C) = 1.80 Å, r(C–O) = 1.30 Å, ϕ(Im–Fe–C) = 167.0°, and ϕ(Fe–C–O) = 180.0°. These numbers are based on the results of X-ray and neutron crystallographic studies on (carbon monoxy)HbA and -Mb (Baldwin, 1980; Norvell et al., 1975). The Urey-Bradley force field was used for the potential function, and the force constants used were transferred from similar systems with a slight adjustment for best fit. These force constants (in mdyn/Å) are K(Fe–Im) = 1.33, K(Fe–C) = 2.85, K(C–O) = 15.80,

Table I: Comparison of Observed and Calculated Frequencies in HbCO

no.	$^{12}C^{16}O$	$^{13}C^{16}O$ (shift)	$^{12}C^{18}O$ (shift)	$^{13}C^{18}O$ (shift)	assignment[a]
		(A) Observed Frequencies (cm^{-1})			
ν_1	1951	1908 (43)	1908 (43)	1861 (90)	ν(C–O)
ν_2	578	*563 (15)*	*576 (2)*	560 (18)	δ(Fe–C–O)
ν_3	507	503 (4)	498 (9)	494 (13)	ν(Fe–C)
		(B) Calculated Frequencies (cm^{-1}), Based on the Model Im–Fe–C–O			
ν_1	1948	1904 (44)	1905 (43)	1858 (90)	
ν_2	579	*561 (18)*	*574 (5)*	556 (23)	
ν_3	507	502 (5)	496 (11)	491 (16)	
		(C) Calculated Frequencies (cm^{-1}), Based on the Model Im–Fe–O–C			
ν_1	1947	1904 (43)	1899 (48)	1856 (91)	
ν_2	576	*570 (6)*	*554 (22)*	548 (28)	
ν_3	506	501 (5)	495 (11)	490 (16)	

[a] ν(A–B), stretching of bond A–B; δ(A–B–C), bending of bond angle A–B–C.

H(Im–Fe–C) = 0.57, H(Fe–C–O)$_{\text{in plane}}$ = 0.50, and H(Fe–C–O)$_{\text{out of plane}}$ = 0.50. Stretching–stretching interaction force constants between two adjacent bonds are F[(Im–Fe)–(Fe–C)] = 0.10 mdyn/Å and F[(Fe–C)–(C–O)] = 1.20 mdyn/Å. The deformation–deformation interaction between two angles was neglected in the calculations. The normal mode analysis was performed according to Wilson's GF-matrix method (Wilson et al., 1955). There are a total of six normal vibrations in this model, and each normal vibration was defined in terms of the following internal coordinate: $R_1 = \nu$(Im–Fe), $R_2 = \nu$(Fe–C), $R_3 = \nu$(C–O), $R_4 = \delta$(Im–Fe–C), $R_5 = \delta_{\text{in plane}}$(Fe–C–O), and $R_6 = \delta_{\text{out of plane}}$(Fe–C–O). Listed in Table I are the observed and calculated frequencies. The pattern of isotope shifts for $^{13}C^{16}O$, $^{12}C^{18}O$, and $^{13}C^{18}O$ agrees well between observed and calculated values.

There may be a question of whether the carbon atom indeed binds directly to iron (Alben & Caughey, 1968). Normal coordinate analysis, based on the model Im–Fe–O–C, has been performed with its results also listed in Table I. The structural parameters are the same except for the exchange of carbon and oxygen. To fit the experimentally observed frequencies, we have used the following force constants (in mdyn/Å): K(Fe–Im) = 1.33, K(Fe–O) = 2.60, K(O–C) = 15.80, H(Im–Fe–O) = 0.57, H(Fe–O–C)$_{\text{in plane}}$ = 1.1, H(Fe–O–C)$_{\text{out of plane}}$ = 1.1, F[(Im–Fe)–(Fe–O)] = 0.1, and F[(Fe–O)–(O–C)] = 1.2. It is readily seen that the isotope shifts for ν_2 (Table I) based on this model do not agree with the observed ones. This may be taken as independent evidence that carbon rather than oxygen binds directly to iron in (carbon monoxy)HbA and -Mb.

Careful examination of lower frequency region spectra reveals additional important information. (1) The line width of the ν(Fe–CO) mode in (carbon monoxy)Mb is considerably greater than that of (carbon monoxy)HbA, indicating multiple ν(Fe–CO) stretching frequencies, consistent with the multiple ν(C–O) stretching frequencies observed by IR spectroscopy and in our Raman study. Multiple ν(C–O) frequencies have been ascribed to three heme–carbonyl conformers due to different local environments of the iron–carbonyl group (Makinen et al., 1979). (2) The porphyrin ring mode at ~586 cm^{-1} in Mb$^{12}C^{16}O$ and Mb$^{12}C^{18}O$ exhibits an anomalous intensity increase (see Figure 6) which is presumably caused by being too close to the δ(Fe–C–O) bending vibration at ~576 cm^{-1} (weak resonance interaction, resulting in intensity borrowing).

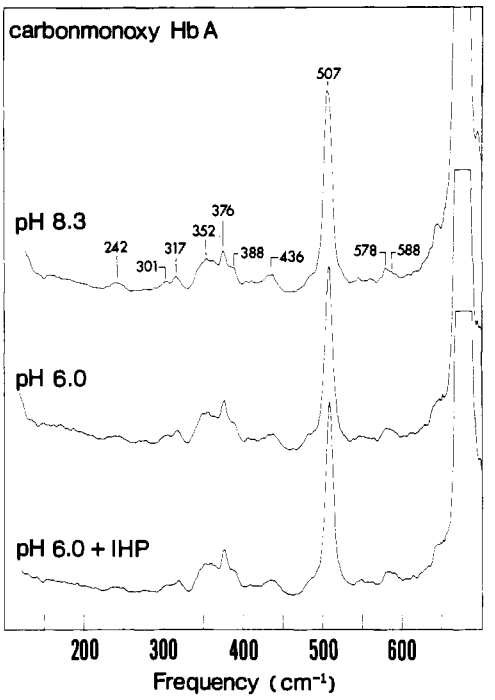

FIGURE 7: pH and IHP effects on the lower frequency region (100–700 cm^{-1}) spectra of (carbon monoxy)HbA. Conditions were ~60 μM (carbon monoxy)HbA (heme basis) in 0.05 M Tris-HCl, pH 8.4, buffer (upper spectrum), 0.05 M citrate–phosphate, pH 6.0, buffer (middle spectrum), and 0.05 M citrate–phosphate, pH 6.0, buffer in the presence of IHP (10 mM) (lower spectrum). Other conditions are the same as in Figure 1.

Quaternary Structure Change. The effect of quaternary structure change on the strength of the Fe–ligand bond is of particular importance in understanding the nature of cooperative oxygen binding to hemoglobin. In the absence of bonding geometry change, the Fe–ligand stretching frequency is a measure of the Fe–ligand bond strength. Here, we examined the influence of the quaternary structure change on ν(Fe–CO) in (carbon monoxy)hemoglobin, which may be considered as an ideal model for oxyhemoglobin. Human oxy-HbA and (carbon monoxy)HbA are known to be in the R quaternary structure even in the presence of inositol hexaphosphate (IHP) (Perutz et al., 1976). In Figure 7, we present the resonance Raman spectra (100–700 cm^{-1}) of (carbon monoxy)HbA at pH 8.3 (upper spectrum), 6.0 (middle spectrum), and 6.0 (lower spectrum) with IHP. These three spectra are essentially identical, i.e., no noticeable changes (within ±1 cm^{-1}) in ν(Fe–CO) and δ(Fe–C–O). Examination of the ν(C–O) mode at 1951 cm^{-1} under the same conditions also revealed no detectable changes, as expected. Somewhat unexpected was the observation that addition of IHP also produced no detectable effect on the (carbon monoxy)Hb Kansas spectrum (Figure 8), although Kincaid et al. (1979) reported a small decrease (~0.7 cm^{-1}) in the IR ν(C–O) frequency. Hb Kansas is an interesting human Hb variant whose quaternary structure can be switched in its ligated forms from the R to the T state by IHP (Ogawa et al., 1972; Gibson et al., 1973; Anderson, 1975; Kilmartin et al., 1978). Under our experimental conditions (heme concentration ~100 μM), some dimer formation (as much as 50%) may be expected (Atha et al., 1979). However, the absence of asymmetric line broadening at 507 cm^{-1} led us to conclude that the ν(Fe–CO) vibration (hence the Fe–C bond strength) is the same in both

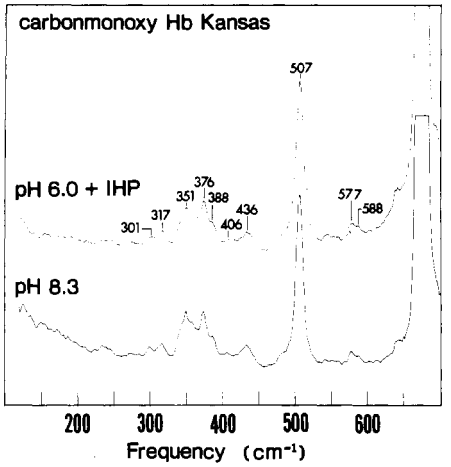

FIGURE 8: pH and IHP effects on the lower frequency region (100–700 cm^{-1}) spectra of (carbon monoxy)Hb Kansas. Conditions were ~100 μM (carbon monoxy)Hb Kansas (heme basis) in 0.05 M citrate–phosphate, pH 6.0, buffer in the presence of IHP (10 mM) (upper spectrum) and 0.05 M Tris-HCl, pH 8.4, buffer (lower spectrum). Other conditions are the same as in Figure 1.

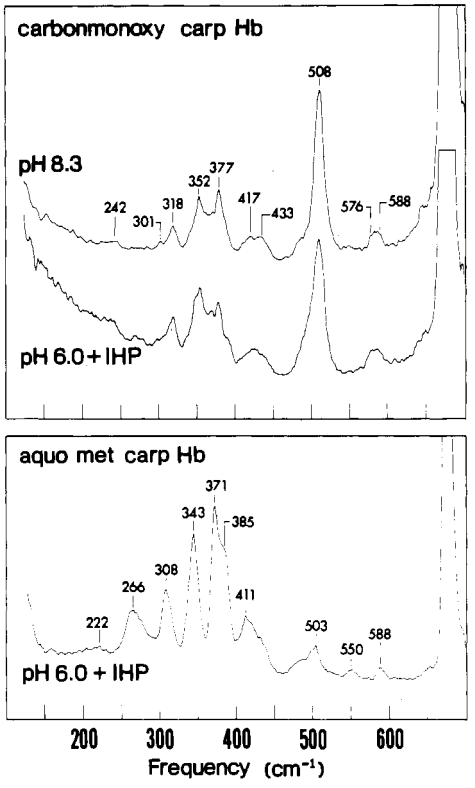

FIGURE 9: pH and IHP effects on the lower frequency region (100–700 cm^{-1}) spectra of carp (carbon monoxy)Hb (upper panel). Conditions were ~60 μM carp (carbon monoxy)Hb (heme basis) in 0.05 M Tris-HCl, pH 8.4, buffer (upper spectrum) and 0.05 M citrate–phosphate, pH 6.0, buffer in the presence of IHP (2.4 mM) (lower spectrum). Other conditions are the same as in Figure 1. Lower frequency region (100–700 cm^{-1}) spectra of carp aquomet-Hb in 0.05 M citrate–phosphate, pH 6.0, buffer in the presence of IHP (2.5 mM). Other conditions are the same as in Figure 1 (lower panel).

R and T forms. Thus, no significant change in either Fe–C or C–O bond energy is induced by switching the quaternary structure from the R to the T form in ligated (carbon monoxy)Hb Kansas. The absence of bond tension between the iron atom and the proximal histidine is also suggested (see Discussion).

Carp Hb is another interesting hemoglobin which is a mixture of three components; its quaternary structure in the

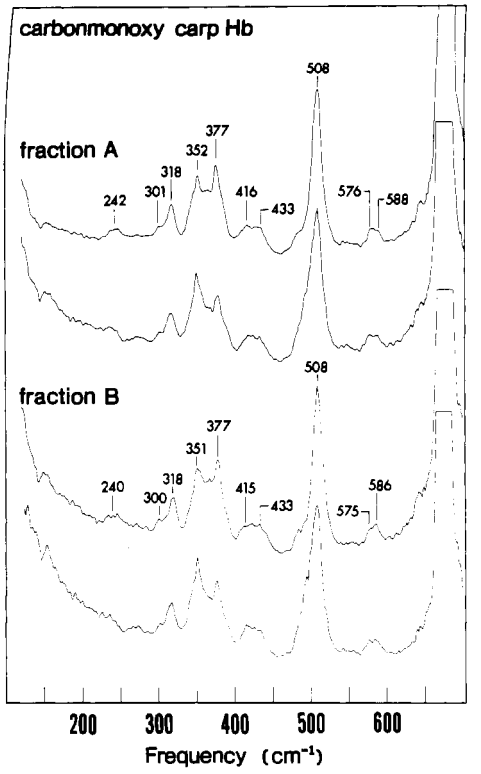

FIGURE 10: pH and IHP effects on lower frequency region (100–700 cm^{-1}) spectra of carp (carbon monoxy)Hb fraction A (upper portion) and fraction B (lower portion). Conditions were 60 μM carp (carbon monoxy)Hb (heme basis) in 0.05 M Tris-HCl, pH 8.4, buffer (upper spectra of each portion) and in 0.05 M citrate–phosphate, pH 6.0, buffer in the presence of IHP (2.5 mM) (lower spectra of each portion). Other conditions are the same as in Figure 1.

ligated state can also be converted to the T structure upon addition of IHP at lower pH, even in relatively low protein concentration, and the addition of IHP stabilizes the ligated molecule completely in the T structure (Tan et al., 1972, 1973; Tan & Noble, 1973; Pennelly et al., 1975). In Figure 9 are shown the spectra (100–700 cm^{-1}) of carp HbCO at pH 8.3 and 6.0 (with IHP). Without IHP, the ν(Fe–CO) mode at 508 cm^{-1} exhibited a very slight broadening when the pH was changed from 8.3 to 6.0. However, the addition of IHP (2.4 mM) at pH 6.0 induced a more pronounced broadening on the lower energy side of the ν(Fe–CO) mode (see Figure 9, upper panel). The results suggest the presence of a new conformer (or conformers). To make sure that this broadening was not caused by partial oxidation of the heme, we obtained resonance Raman spectra of carp aquomet-Hb with IHP at pH 6.0 for comparison (Figure 9, lower panel). In addition, we separated the three components of carp Hb [denoted as fractions A, B, and C following the notation of Tan et al. (1972)] and examined their resonance Raman spectra. It is concluded that the broadening of the ν(Fe–CO) stretching from the R to the T state is common to all three components. Figure 10 shows only results from fractions A and B.

Discussion

Porphyrin Ring Vibrations. Soret and Q (α and β) absorption bands are due to π–π^* transitions in the porphyrin from the a_{1u} and a_{2u} to the e^*_g orbitals (Gouterman, 1961; Zerner et al., 1966), and the $a_{1u} \rightarrow e^*_g$ and $a_{2u} \rightarrow e^*_g$ transitions have similar transition dipoles so that their intrinsic intensities before mixing are also similar. Since the two transition moments belong to the same representation of the symmetry group (E_u), these two states can be mixed by configuration interaction. Of the two new excited states, the

higher energy state generates the Soret band while the lower energy state gives rise to the Q (α and β) bands. Based on symmetry, e^*_g can interact with the d_π orbitals (d_{xz} and d_{yz}) through back-donation, and as a result, charge is transferred from the metal orbital to the porphyrin π^* orbitals.

Although the gross electronic structure of heme is similar in (carbon monoxy)Hb and oxy-Hb, the frequencies and relative intensities of the corresponding lines are somewhat different, as first noticed by Rimai et al. (1975). Several porphyrin ring modes (1372, 1471, 1498, and 1633 cm^{-1}) in the spectrum of (carbon monoxy)HbA exhibit lower frequencies than those corresponding modes (1377, 1473, 1506, and 1640 cm^{-1}) in the oxy-Hb spectrum. This may be explained by the extent of the d_π(Fe)–π^*(porphyrin) interaction; the frequencies are raised when the axial ligands are replaced by better π acceptors, which compete with the porphyrin π^* orbitals for the d_π(Fe) electrons.

Since the lowest empty orbital of CO is relatively higher than $\pi^*(O_2)$ orbitals in energy, the interaction between d_π(Fe) and π^*(CO) is weaker than that between d_π(Fe) and $\pi^*(O_2)$, causing stronger interaction between d_π(Fe) and π^*(porphyrin). Thus, the resulting higher electron population in π^* porphyrin orbitals leads to lower frequencies of porphyrin ring modes in (carbon monoxy)Hb.

Fe–CO Stretching Vibration. Through the d_π(Fe)–π^*(porphyrin) orbital interaction, the electronic excitation at the porphyrin ring by the illumination of laser light at the Soret or Q (α and β) bands can affect the d_π(Fe)–π^*(ligand) interaction indirectly, leading to the photodissociation of the sixth ligand. The external ligands such as NO, CO, or O_2, or alkyl isocyanide are bound to heme iron(II) through the d_π(Fe)–π^*(ligand) interaction in addition to the d_{z^2}(Fe)–π^*(ligand) interaction (Kitagawa et al., 1976; Tsubaki & Yu, 1981), whereas ligands such as CN, N_3, and imidazole ligate to the heme iron(III) almost entirely by the d_{z^2}(Fe)–lone-pair(ligand) interaction. Thus, "ferric-like" reduced hexacoordinated Hbs [such as oxy-Hb, (carbon monoxy)Hb, and nitrosyl-Hb] are known to be photodissociable more or less, while low-spin oxidized derivatives are photoinsensitive. The difference in photodissociability among oxy-Hb, (carbon monoxy)Hb, nitrosyl-Hb, and (alkyl isocyanide)Hb is presumably due to the relative degree of contribution of the d_π(Fe)–π^*(ligand) interaction in the Fe–ligand bond. As mentioned in the preceding section, the absolute strength of the d_π(Fe)–π^*(CO) interaction itself is smaller than that of the d_π(Fe)–$\pi^*(O_2)$ interaction, but the d_{z^2}(Fe)–lone-pair(ligand) interaction, which is a primary interaction in the Fe–O_2 bond, is so weak in the Fe–CO bond because of bonding geometry that the contribution of the d_π(Fe)–π^*(CO) interaction in the Fe–CO bond is much larger that that of d_π(Fe)–$\pi^*(O_2)$ in the Fe–O_2 bond. Indeed, this may be the reason why (carbon monoxy)Hb is the most photodissociable among the ferric-like reduced hexacoordinated Hbs.

Since O_2 is both a better π acceptor and σ donor than CO, one would expect a stronger Fe–O bond. This is consistent with the observation that the ν(Fe–O_2) stretching frequency ($\sim$570 cm^{-1}) is higher than the ν(Fe–CO) stretching frequency ($\sim$507–512 cm^{-1}).[1] This may seem paradoxical since the affinity for CO is much higher than that for O_2. The difficulty is removed when one considers the charge reorganization among several bonds (i.e., C–O bond, Fe–proximal histidine, and porphyrin skeleton) upon ligand binding. Since the overall free-energy change associated with ligand binding, which determines the binding affinity, is not localized at the iron–ligand bond, the iron–ligand bond strength alone may not be a good indication of binding affinity. In fact, E. A. Kerr, H. C. Mackin, and N.-T. Yu (unpublished experiments) found that the ν(Fe–CO) for low-affinity Fe^{II}(TpivPP)(1,2-Me_2Im) is higher than that for the high-affinity Fe^{II}(TpivPP)(1-MeIm), whereas the ν(Fe–O_2) is lower for the low-affinity heme.

Preliminary studies of excitation profiles of the Fe–ligand stretching modes such as ν(Fe–O_2), ν(Fe–CO), and ν(Fe–NO) revealed that these modes can be enhanced everywhere from the Soret to the α band, and their Raman intensities follow the profiles of visible absorption spectra (M. Tsubaki and N.-T. Yu, unpublished results). This phenomenon can be easily understood if one considers the importance of the d_π(Fe)–π^*(ligand) interaction which is indirectly influenced by the electronic configuration change in the porphyrin ring through the d_π(Fe)–π^*(porphyrin) interaction. Laser excitation into the $\pi \rightarrow \pi^*$ porphyrin transition may lead to the elongation (or dissociation) of the Fe–CO bond in the excited state, which should be effective in shifting the origin of the potential energy curve along this coordinate. Thus, through the Franck-Condon scattering mechanism, we have observed the resonance enhancement of the Fe–CO stretching vibration (Felton & Yu, 1978). In this regard, the strong Raman intensity of the Fe–CO stretching mode might be a good indicator for the extent of the relative contribution of the d_π(Fe)–π^*(CO) interaction in the Fe–CO bond.

Fe–C–O Bending Vibration. The δ(Fe–C–O) bending vibration at $\sim$577 cm^{-1} detected in our present study of (carbon monoxy)Hb-Mb adds an interesting dimension to the CO binding studies. Both intensity and frequency are expected to be sensitive to the CO bonding geometry, i.e., linear perpendicular, linear tilted, or bent with varying Fe–C–O angles. At present, there are still some questions about the detailed Fe–CO geometry in carbon monoxy hemoproteins (Huber et al., 1970; Heidner et al., 1976; Norvell et al., 1975; Steigemann & Weber, 1979; Padlan & Love, 1975; Baldwin, 1980). Resonance Raman techniques may become a powerful tool to probe the exact nature of the bending or tilting of the coordinated CO ligand.

Another interesting aspect of the δ(Fe–C–O) bend is its position relative to the ν(Fe–CO) stretch. In MbCO and HbCO, the ν(Fe–C–O) bend appears at $\sim$577 cm^{-1}, which is higher than the ν(Fe–CO) stretch at $\sim$510 cm^{-1}. However, in a nonheme Fe–CO system, it is known that the δ(Fe–C–O) frequency is lower than the ν(Fe–CO) frequency (Kroeker et al., 1980).

Carp (Carbon monoxy)Hb and Quaternary Structure Change. At neutral pH, carp Hb exhibits the usual cooperative ligand binding, characteristic of the T $\rightarrow$ R quaternary structure transition. At lower pH ($\sim$6.0), in the presence of organic phosphate such as IHP, both liganded and unliganded derivatives adopt the T structure according to equilibrium and kinetic studies (Tan et al., 1972, 1973; Tan & Noble, 1973; Pennelly et al., 1975). Thus, this Hb provides a good opportunity for examining the effects of quaternary structure change on heme-associated vibrations, particularly the iron–ligand stretching mode by resonance Raman spectroscopy.

The iron–ligand stretching frequency provides the most valuable and direct information about the nature of the heme–ligand interaction. This frequency is expected to respond to any changes in electron donation to the iron. Of particular

[1] Comparison of force constants for Fe–C and Fe–O bonds in hemoproteins is difficult because of the uncertainty in CO bonding geometry. However, in the Fe(II) "picket fence" system, the force constants are estimated as 2.61 mdyn/Å for the Fe–O bond and 2.51 mdyn/Å for the Fe–C bond.

interest is the sensitivity of this vibration to bond tension between the iron atom and the proximal histidine. E. A. Kerr, H. C. Mackin, and N.-T. Yu (unpublished experiments) studied the effect of proximal tension on the ν(Fe–CO) frequency in the CO complexes of Fe(II) "picket fence" porphyrin, Fe^{II}(TpivPP). When the proximal base is changed from 1-methylimidazole (unhindered) to 1,2-dimethylimidazole (sterically hindered), the ν(Fe–CO) increases from 489 to 496 cm^{-1} (in benzene). In the case of oxy complexes, they found a reverse effect; i.e., the proximal tension is to decrease the ν(Fe–O_2) from 571 to 565 cm^{-1} (also in benzene). This confirms the earlier report by Walters et al. (1980) that there is a 4-cm^{-1} difference in ν(Fe–O_2) between Fe^{II}(TpivPP)(1-MeIm)(O_2) and Fe^{II}(TpivPP)(1,2-Me_2Im)(O_2) (in CH_2Cl_2). In contrast, Hori & Kitagawa (1980) found the insensitivity of ν(Fe–O_2) to such a proximal tension in the same heme system.

Carbon monoxide is an excellent resonance Raman visible ligand for studying the effects of quaternary structure change because the ν(Fe–CO) stretching mode is very strong in the resonance Raman spectra. The observed asymmetric broadening on the lower energy side of the ν(Fe–CO) mode in the T state of carp HbCO (see Figure 9) is a very interesting phenomenon. What can be the cause of this broadening? We have definitely ruled out the possibilities of partial oxidation, contribution of deoxy species, and formation of intermediate photoproducts. The spectral features are independent of laser power (5–30 mW), the addition of excess sodium dithionite, and the rotating speed of our Raman cell (500–2000 rpm). It appears that in the T-state carp HbCO there is a small fraction of a minor conformer (or conformers) with a weaker Fe–CO bond or a somewhat different CO distortion in equilibrium with the major conformer which has the same Fe–CO bond as in the R state. If the broadening were caused by the proximal base tension, one would expect it to appear on the higher energy side instead of the lower energy side as is actually observed. This implies that there is no appreciable Fe–N_ϵ(His F8) bond tension in the T-state carp HbCO. At present, no complete data are available on the factors affecting the ν(Fe–CO) frequency. However, recent studies in this laboratory on "strapped" hemes with steric hindrance on the distal side (Ward et al., 1981) revealed that the ν(Fe–CO) frequency is lower with less CO distortion (in collaboration with Professor C. K. Chang, Michigan State University).

Additional evidence for the absence of *localized bond tension* in the T-state Hb is provided by the work of Nagai et al. (1980a,b), who observed that the ν(Fe–O_2) frequency is the same between the R state (oxy-HbA) and the T state (oxy-Hb Kansas and oxy-HbM Milwaukee in the presence of IHP at low pH). Comparison of ν(Fe–O_2) in the R and T states of carp Hb is difficult because carp oxy-Hb is readily oxidized in the presence of IHP at lower pH (Mayo & Chien, 1979). Our studies on the T-state (carbon monoxy)Hb Kansas (Figure 8) also indicate the absence of localized bond tension between the heme iron and proximal histidine.

Finally, the insensitivity of the iron–ligand vibration to quaternary structure change was also found in carp cyanomet-Hb. The Fe(III)–CN stretching vibration, identified at 455 cm^{-1} by the isotope, did not exhibit any noticeable change upon R $\rightarrow$ T conversion (M. Tsubaki and N.-T. Yu, unpublished experiments). However, we do not know at present if the ν(Fe–CN) frequency is sensitive to the proximal base tension.

Added in Proof

M. A. Walters and T. G. Spiro (unpublished results) also found that the Raman intensity of ν(Fe–O_2) follows the profile of the HbO_2 absorption spectrum. They came to the same conclusion that its intensity is due to coupling with the porphyrin π–π^* electronic transitions, resulting in A-term (Franck-Condon) resonance Raman scattering. We thank Professor Spiro for communicating the results prior to publication.

References

Alben, J. O., & Caughey, W. S. (1968) *Biochemistry 7*, 175.

Anderson, L. (1975) *J. Mol. Biol. 94*, 33.

Asher, S. A., Vickery, L. E., Schuster, T. M., & Sauer, K. (1977) *Biochemistry 16*, 5849.

Atha, D. H., Johnson, M. L., & Riggs, A. F. (1979) *J. Biol. Chem. 254*, 12390.

Baldwin, J. M. (1980) *J. Mol. Biol. 136*, 103.

Brunner, H. (1974) *Naturwissenschaften 61*, 129.

Caughey, W. S., Alben, J. O., McCoy, S., Boyer, S. H., Charache, S., & Hathaway, P. (1969) *Biochemistry 8*, 59.

Chottard, G., & Mansuy, D. (1977) *Biochem. Biophys. Res. Commun. 77*, 5849.

Coppey, M., Tourbez, H., Valat, P., & Alpert, B. (1980) *Nature (London) 284*, 568.

Dallinger, R. F., Nestor, J. R., & Spiro, T. G. (1978) *J. Am. Chem. Soc. 100*, 6252.

Felton, R. H., & Yu, N.-T. (1978) in *The Porphyrins* (Dolphin, D., Ed.) Vol. III, Chapter VIII, Academic Press, New York.

Friedman, J. M., & Lyons, K. B. (1980) *Nature (London) 284*, 570.

Gibson, Q. H., Riggs, A., & Inamura, T. (1973) *J. Biol. Chem. 248*, 5976.

Gouterman, M. (1961) *J. Mol. Spectrosc. 6*, 138.

Heidner, E. J., Ladner, R. C., & Perutz, M. F. (1976) *J. Mol. Biol. 104*, 707.

Hori, H., & Kitagawa, T. (1980) *J. Am. Chem. Soc. 102*, 3608.

Huber, R., Epp, O., & Formanek, H. (1970) *J. Mol. Biol. 52*, 349.

Kilmartin, J. V., Hewitt, J. A., & Wooton, J. F. (1975) *J. Mol. Biol. 93*, 203.

Kilmartin, J. V., Anderson, N. L., & Ogawa, S. (1978) *J. Mol. Biol. 123*, 71.

Kincaid, J. R., Spiro, T. G., Valentine, J. S., Saperstein, D. D., & Rein, A. J. (1979) *Inorg. Chim. Acta 33*, L181.

Kitagawa, T., Kyogoku, Y., Iizuka, T., & Saito, M. I. (1976) *J. Am. Chem. Soc. 98*, 5169.

Kroeker, R. M., Hansma, P. K., & Kaska, W. C. (1980) *J. Chem. Phys. 72*, 4845.

Lyons, K. B., Friedman, J. M., & Flenry, P. A. (1978) *Nature (London) 275*, 566.

Makinen, M. W., Houtchens, R. A., & Caughey, W. S. (1979) *Proc. Natl. Acad. Sci. U.S.A. 76*, 6042.

Mayo, K. H., & Chien, J. C. W. (1979) *Biochim. Biophys. Acta 581*, 44.

Nagai, K., Kitagawa, T., & Morimoto, H. (1980a) *J. Mol. Biol. 136*, 271.

Nagai, K., Enoki, Y., & Kitagawa, T. (1980b) *Biochim. Biophys. Acta 624*, 304.

Noble, R. W., Brunori, M., Wyman, J., & Antonini, E. (1967) *Biochemistry 6*, 1216.

Norvell, J. C., Nunes, A. C., & Schoenborn, B. P. (1975) *Science (Washington, D.C.) 190*, 568.

Nozaki, Y., & Tanford, C. (1967) *Methods Enzymol. 11*, 733.

Ogawa, S., Mayer, A., & Shulman, R. G. (1972) *Biochem. Biophys. Res. Commun. 49*, 1485.

Padlan, E. A., & Love, W. E. (1975) *J. Biol. Chem. 249*, 4067.

Pennelly, R. R., Tan-Wilson, A. L., & Noble, R. W. (1975) *J. Biol. Chem. 250*, 7239.
Perutz, M. F., Kilmartin, J. V., Nagai, K., Szabo, A., & Simon, S. R. (1976) *Biochemistry 15*, 378.
Rimai, L., Salmeen, I., & Petering, D. H. (1975) *Biochemistry 14*, 378.
Satterlee, J. D., Teintze, M., & Richards, J. H. (1978) *Biochemistry 17*, 1457.
Sawicki, C. A., & Gibson, Q. H. (1979) *J. Biol. Chem. 254*, 4058.
Stanford, M. A., Swartz, J. C., Phillips, T. E., & Hoffman, B. M. (1980) *J. Am. Chem. Soc. 102*, 4492.
Steigemann, W., & Weber, E. (1979) *J. Mol. Biol. 127*, 309.
Tan, A. L., & Noble, R. W. (1973) *J. Biol. Chem. 248*, 7412.
Tan, A. L., De Young, A., & Noble, R. W. (1972) *J. Biol. Chem. 247*, 2493.
Tan, A. L., Noble, R. W., & Gibson, Q. H. (1973) *J. Biol. Chem. 248*, 2880.
Terner, J., Spiro, T. G., Nagumo, M., Nicol, M. F., & El-Sayed, M. A. (1980) *J. Am. Chem. Soc. 102*, 3238.
Tsubaki, M., & Yu, N.-T. (1981) *Proc. Natl. Acad. Sci. U.S.A. 78*, 3581.
Tsubaki, M., Srivastava, R. B., & Yu, N.-T. (1981) *Biochemistry 20*, 946.
Tucker, P. W., Phillips, S. E. V., Perutz, M. F., Houtchens, R. A., & Caughey, W. S. (1978) *Proc. Natl. Acad. Sci. U.S.A. 76*, 1076.
Walters, M. A., Spiro, T. G., Suslick, K. S., & Collman, J. P. (1980) *J. Am. Chem. Soc. 102*, 6857.
Ward, B., Wang, C. B., & Chang, C. K. (1981) *J. Am. Chem. Soc. 103*, 5236.
Wilson, E. B., Jr., Decius, J. C., & Cross, P. C. (1955) *Molecular Vibrations*, McGraw-Hill, New York.
Woodruff, W. H., & Farquharson, S. (1978) *Science (Washington, D.C.) 201*, 833.
Wright, P. G., Stein, P., Burke, J. M., & Spiro, T. G. (1979) *J. Am. Chem. Soc. 101*, 3531.
Yu, N.-T. (1977) *CRC Crit. Rev. Biochem. 4*, 229.
Yu, N.-T., & Srivastava, R. B. (1980) *J. Raman Spectrosc. 9*, 166.
Yu, N.-T., & Tsubaki, M. (1980) *Biochemistry 19*, 4647.
Zerner, M., Gouterman, M., & Kobayashi, H. (1966) *Theor. Chim. Acta 6*, 363.

Resonance Raman Investigation of Nitric Oxide Bonding in Nitrosylhemoglobin A and -myoglobin: Detection of Bound N–O Stretching and Fe–NO Stretching Vibrations from the Hexacoordinated NO–Heme Complex†

Motonari Tsubaki‡ and Nai-Teng Yu*

ABSTRACT: With excitation at 406.7 nm, we have observed the resonance Raman enhancement of the bound ν(N–O) stretch at $\sim$1623 cm^{-1} in nitrosylhemoglobin A and nitrosylmyoglobin, indicating the existence of a charge-transfer transition underlying the strong Soret band. The ν(Fe–NO) stretch at 551 cm^{-1} has also been detected in the Soret as well as in the Q-band region, a phenomenon similar to the ν(Fe–O_2) and ν(Fe–CO) stretches in oxy and carbon monoxy hemoproteins. It appears that these iron–ligand vibrations may be resonance enhanced via porphyrin $\pi \rightarrow \pi^*$ transitions. Upon addition of inositol hexaphosphate at pH 6.0, the ν(Fe–NO) stretch at 551 cm^{-1} and a low-frequency mode at 301 cm^{-1} exhibit an intensity decrease by approximately one-half. Contrary to the work of Stong et al. [Stong, J. D., Burke, J. M., Daly, P., Wright, P., & Spiro, T. G. (1980) *J. Am. Chem. Soc. 102*, 5815], who employed an excitation wavelength at 454.5 nm, we observed no intensity increase at 592 cm^{-1} attributable to the ν(Fe–NO) stretch from the pentacoordinated NO–heme complex in the α subunits.

Nitric oxide (NO) has been employed as a probe to detect the conformational change of the heme moiety in hemoglobin (Hb) when the quaternary structure is switched from the R to the T form (Rein et al., 1972; Cassoly, 1974; Taketa et al., 1975; Maxwell & Caughey, 1976; Perutz et al., 1976). Electron paramagnetic resonance (EPR) studies revealed that human nitrosylhemoglobin A (nitrosyl-HbA) in the R structure has four hexacoordinated hemes, whereas in the T structure, as induced by inositol hexaphosphate (IHP), it is a hybrid of penta- and hexacoordinated NO–heme complexes (Maxwell & Caughey, 1976; Perutz et al., 1976). Supporting evidence has come from both infrared (IR) and resonance Raman spectroscopic studies. Bound NO in the R structure of nitrosyl-HbA gives rise to a single IR absorption band at 1615 cm^{-1}, characteristic of the ν(N–O) stretch in a hexacoordinated NO–heme, and addition of IHP causes the appearance of a second IR band at 1668 cm^{-1}, characteristic of the ν(N–O) stretch in a pentacoordinated NO–heme (Maxwell & Caughey, 1976). On the other hand, the resonance Raman spectrum of nitrosyl-HbA displays a depolarized porphyrin ring mode at 1633 cm^{-1}; half of its intensity is shifted to 1644

† From the School of Chemistry, Georgia Institute of Technology, Atlanta, Georgia 30332. *Received June 1, 1981.* This research was supported by Grant GM 18894 from the National Institutes of Health. N.-T.Y. is the recipient of National Institutes of Health Research Career Development Award (EY 00073).

‡ Present address: Department of Biochemistry, Kagawa Medical School, Kagawa 761-07, Japan.

0006-2960/82/0421-1140$01.25/0